



TITLE:

# Mössbauer Effect of Fe in Fe(OH) (Physical and Inorganic Chemistry)

AUTHOR(S):

Miyamoto, Hiroki; Shinjo, Teruya; Bando,  
Yoshichika; Takada, Toshio

---

CITATION:

Miyamoto, Hiroki ...[et al]. Mössbauer Effect of Fe in Fe(OH) (Physical and Inorganic Chemistry). Bulletin of the Institute for Chemical Research, Kyoto University 1968, 45(4-5): 333-341

ISSUE DATE:

1968-01-20

URL:

<http://hdl.handle.net/2433/76208>

RIGHT:

# Mössbauer Effect of $\text{Fe}^{57}$ in $\text{Fe}(\text{OH})_2$

Hiroki MIYAMOTO, Teruya SHINJO, Yoshichika BANDO  
and Toshio TAKADA\*

(Takada Laboratory)

Received August 31, 1967

The Mössbauer effect of  $\text{Fe}(\text{OH})_2$  was measured in paramagnetic and antiferromagnetic region (4.2°K). At 90°K, quadrupole splitting  $1/2e^2qQ$  and isomer shift  $\delta$  were observed to be 3.00 mm/sec and 1.25 mm/sec respectively.

As for the spectrum at 4.2°K, four resonance lines were observed in contrast with usual six lines splitting. This spectrum is interpretable in terms of a uniaxial electric field gradient and a magnetic hyperfine field perpendicular to the axis of electric field.

An excellent agreement of experimental hyperfine spectrum with calculated one was obtained by assuming  $\lambda = -0.75$ , where  $\lambda$  is the ratio of the quadrupole interaction energy to the Zeeman one.

The derived values of magnetic hyperfine field,  $1/2e^2qQ$  and  $\delta$  are 200 KOe, 3.06 mm/sec and 1.48 mm/sec respectively at 4.2°K. In consideration of the crystal structure of  $\text{Fe}(\text{OH})_2$ , which is a hexagonal layer structure of  $\text{CdI}_2$  type, spin axis of  $\text{Fe}(\text{OH})_2$  was concluded to be in the  $c$ -plane.

## I. INTRODUCTION

A group of hydroxides of divalent transition metals, such as  $\text{Mn}(\text{OH})_2$ ,  $\text{Fe}(\text{OH})_2$ ,  $\beta\text{-Co}(\text{OH})_2$ , and  $\text{Ni}(\text{OH})_2$ , have the same layer structure of  $\text{CdI}_2$  type. The crystal structure of  $\text{Fe}(\text{OH})_2$  is shown schematically in Fig. 1. This structure consists of the sheets of metal ions separated by two layers of OH ions. Metal ions at octahedral site of OH ions form a hexagonal lattice in a plane normal to the  $c$ -axis. The distance of metal ions between adjacent layers is much longer than

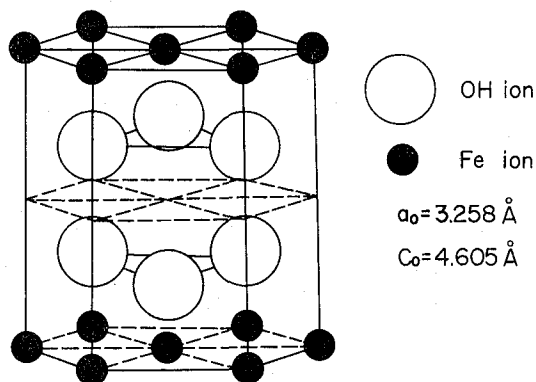


Fig. 1. Crystal structure of  $\text{Fe}(\text{OH})_2$ .

\* 宮本大樹, 新庄輝也, 坂東尚周, 高田利夫

that of them within a layer. Therefore, the magnetic properties of these compounds are expected to be different from a normal antiferromagnetic substance. For example,  $\beta$ - $\text{Co}(\text{OH})_2$ <sup>1,2)</sup> and  $\text{Ni}(\text{OH})_2$ <sup>1,3)</sup> have been reported to show the metamagnetic properties by the authors.

However, research for the magnetic properties of them has been scarcely reported mainly because of difficulties in sample preparation. These hydroxides of divalent ions are apt to change into the oxides or hydroxides of trivalent ions in air. Moreover, it is actually difficult to prepare the sample of large particle size. Particles of  $\text{Fe}(\text{OH})_2$  have the strongest tendency of oxidation among these compounds.

The authors prepared satisfactorily pure sample in nitrogen atmosphere free from oxygen. In the present paper, experimental results of the Mössbauer measurement are described and the magnetic properties of  $\text{Fe}(\text{OH})_2$  are discussed.

## II. EXPERIMENTAL PROCEDURE AND RESULTS

### A. Sample Preparation

$\text{Fe}(\text{OH})_2$  easily changes into oxide or oxyhydrate such as  $\text{Fe}_3\text{O}_4$  or  $\alpha$ ,  $\beta$ ,  $\gamma$ - $\text{FeOOH}$  by oxidation. Therefore, it is necessary to keep the sample free from oxygen during the preparation and measurements.

Ferrous hydroxide was obtained by adding the aqueous solution of alkaline to the aqueous solution of  $\text{FeSO}_4 \cdot 7\text{H}_2\text{O}$ . Aqueous solution of alkaline and  $\text{FeSO}_4 \cdot 7\text{H}_2\text{O}$  free from oxygen were obtained as follows. As shown in Fig. 2, glass vessel-A

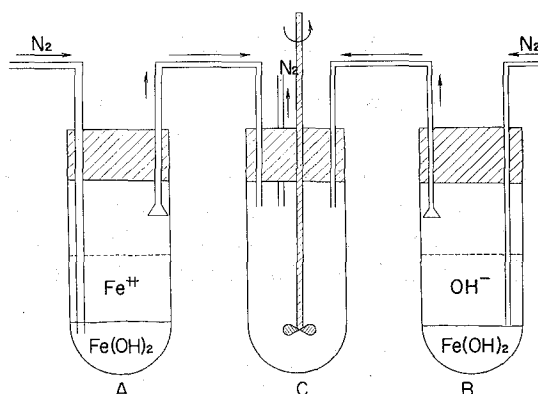
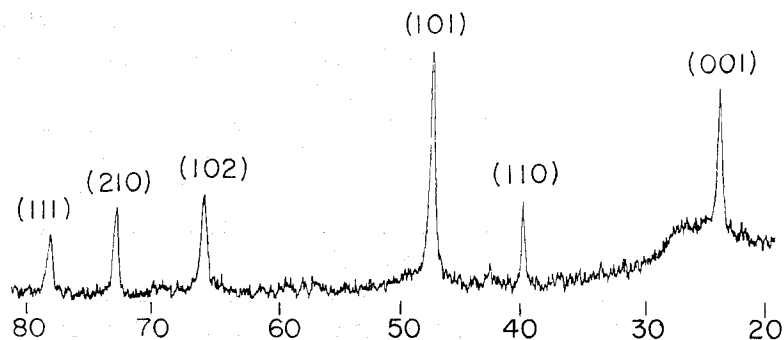


Fig. 2. Schematic illustration of sample preparation system of  $\text{Fe}(\text{OH})_2$  in the nitrogen atmosphere.

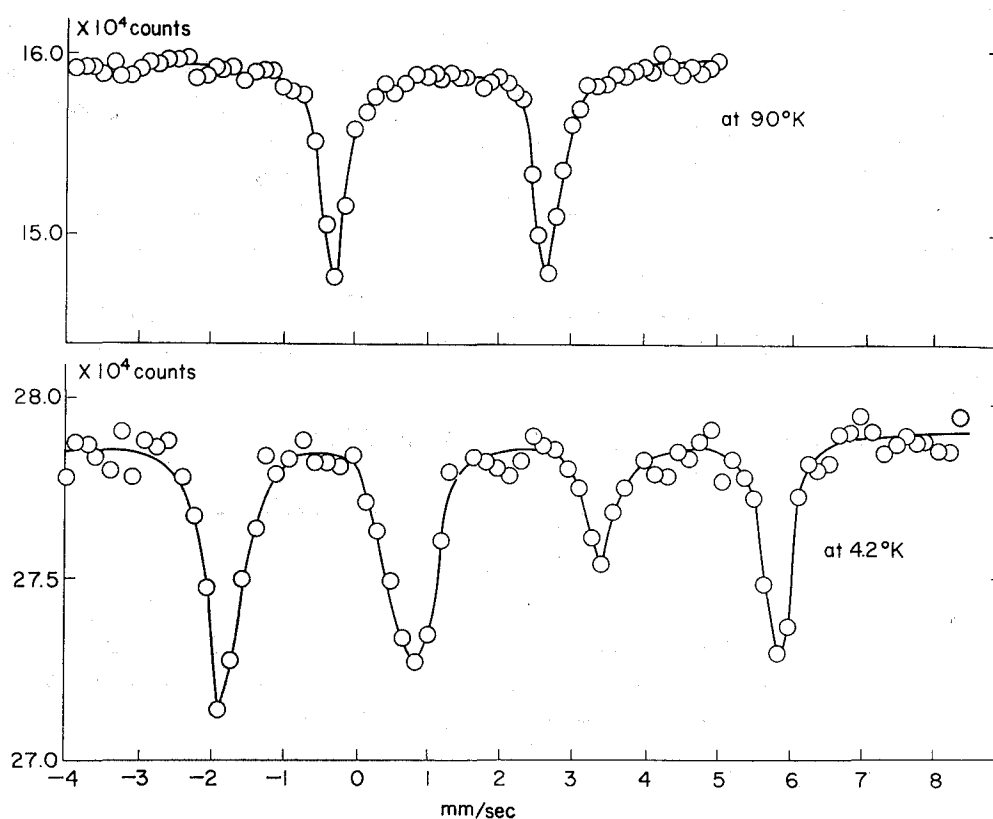
contains 5N- $\text{NaOH}$  solution and vessel-B 1N- $\text{FeSO}_4 \cdot 7\text{H}_2\text{O}$  solution. In vessel-A and B, aqueous solutions, which contained a little amount of  $\text{Fe}(\text{OH})_2$  obtained by the addition of alkaline or ferrous solution, were bubbled by nitrogen gas free from oxygen. In this way, oxygen molecules solved in solution were spent in oxidation of  $\text{Fe}(\text{OH})_2$ . Solutions of the same volume in vessel-A and B were transferred into the vessel-C by gas pressure of nitrogen and could be mixed in the atmosphere free from oxygen. The suspended solution of colloidal  $\text{Fe}(\text{OH})_2$  was stirred at  $70^\circ\text{C}$  for 7 hours to obtain large particles. The sample whose color was white was sealed and transferred into the dry box of nitrogen atmosphere. The sam-

Fig. 3. X-ray diffraction pattern of  $\text{Fe}(\text{OH})_2$ .

ples for X-ray diffraction and Mössbauer measurements were sealed by cellophane tape. The X-ray diffraction pattern measured using  $\text{Fe-K}_\alpha$  radiation shows that the sample is  $\text{Fe}(\text{OH})_2$  and no extra lines exist except broad one due to the cellophane tape. (see Fig. 3) Particle size is obviously larger than  $0.1 \mu$ .

### B. Measurements of Mössbauer Effect and Results

Mössbauer absorption spectra were measured using the TMC commercial set (Gammascope Model 102, Drive Unit Model 305 and Transducer Model 306) operating in time mode. The source was  $\text{Co}^{57}$  doped in Cu metal and kept at room

Fig. 4. Mössbauer spectra of  $\text{Fe}(\text{OH})_2$  at  $90^\circ\text{K}$  and  $4.2^\circ\text{K}$ .

temperature. The velocity was calibrated using iron and stainless steel foils as standard absorbers. Here, isomer shift is represented in comparison with the absorption of stainless steel (conventional origin).

The measurements were carried out between room temperature and 90°K, and at 4.2°K. Figure 4 shows the spectra measured at 90°K and 4.2°K. At the temperature of 90°K the quadrupole splitting and isomer shift were derived to be 3.00 mm/sec and 1.25 mm/sec. No appreciable change of these values was observed in the spectrum of the temperature above 90°K.

The spectrum at 4.2°K consists of four absorption lines in contrast with usual six lines splitting observed in magnetically ordered state. The magnetic susceptibility was measured and represented a sharp maximum at about 34°K. The anomaly in the susceptibility should be originated from the magnetic transition; therefore the spectrum at 4.2°K must be interpreted as the hyperfine structure due to the magnetic and electric quadrupole interactions.

### III. DISCUSSION OF THE MÖSSBAUER SPECTRA

In the paramagnetic region, the magnetic hyperfine field does not exist. Therefore, only the electric field gradient acts on the excited state of  $\text{Fe}^{57}$  nuclei.

In consideration of the crystal structure of  $\text{Fe}(\text{OH})_2$ , the asymmetric factor  $\eta$  of the electric field gradient is thought to be zero and the observed splitting 3.00 mm/sec is due to  $1/2e^2qQ$ .

The large value of the quadrupole splitting is reasonable in consideration of the influence due to the aspherical 3d electron of  $\text{Fe}^{2+}$  ion. In the obtained spectrum, there was not found any absorption due to  $\text{Fe}^{3+}$  ion; therefore the sample was proved to be sufficiently pure. The value of isomer shift, 1.25 mm/sec, is very close to that of completely ionic  $\text{Fe}^{2+}$  ion according to the Walker's analysis. As the spectrum at the paramagnetic region has a doublet of equal intensity, the effect of preferred orientation of particles and anisotropic Mössbauer fraction was neglected in the following discussion.

In the antiferromagnetic state, the magnetic hyperfine field no longer averages to zero. The Hamiltonian of the nuclear spin for the excited state ( $I=3/2$ ) is given by

$$H_e = g_e \mu_N H I_z + \frac{e^2 q Q}{2I(2I-1)} \left\{ \begin{aligned} &\frac{1}{4} (3 \cos^2 \theta - 1) (3 I_z^2 - I(I+1)) \\ &+ \frac{3}{4} \sin \theta \cdot \cos \theta (I_z (I_+ + I_-) + (I_+ + I_-) I_z) \\ &+ \frac{3}{8} \sin^2 \theta (I_+^2 + I_-^2) \end{aligned} \right\} \quad (1)$$

where  $\theta$  is the angle between the direction of magnetic field and the axis of electric field gradient and  $z$  is taken to be parallel to the direction of electron spin.

As for the ground state, the Hamiltonian is given by

$$H_g = g_g \mu_N H \left( I = \frac{1}{2} \right). \quad (2)$$

In the expression of (1) and (2)  $g_e$  and  $g_g$  are gyromagnetic ratio of the excited

and ground state and the values of them are  $-0.100$  and  $+0.180$  respectively.

In order to obtain the hyperfine splitting of the excited state, the secular determinant equation is necessary to be solved.

$$\mathbf{H}\phi = E\phi \text{ or } \mathbf{H} \begin{pmatrix} C_1 \\ C_2 \\ C_3 \\ C_4 \end{pmatrix} = E \begin{pmatrix} C_1 \\ C_2 \\ C_3 \\ C_4 \end{pmatrix} \quad (3)$$

where  $\phi$  is expressed by the linear combination of  $\left|\frac{3}{2}\right\rangle$ ,  $\left|\frac{1}{2}\right\rangle$ ,  $\left|-\frac{1}{2}\right\rangle$  and  $\left|-\frac{3}{2}\right\rangle$ , that is

$$\phi = C_1 \left|\frac{3}{2}\right\rangle + C_2 \left|\frac{1}{2}\right\rangle + C_3 \left|-\frac{1}{2}\right\rangle + C_4 \left|-\frac{3}{2}\right\rangle \quad (4)$$

and the coefficient  $C_i$  must satisfy the following equation,

$$\sum_{i=1}^4 C_i^2 = 1. \quad (5)$$

The secular determinant equation (3) has been solved by Parker's<sup>4)</sup> numerical method. Using his results, it is possible to obtain the energy levels of excited state for the parameter  $\theta$  and  $\lambda$ , where  $\lambda$  is the ratio of quadrupole interaction energy to Zeeman one, that is

$$\lambda = \frac{e^2 q Q / 2I(2I-1)}{g_e \mu_N H}. \quad (6)$$

The energy levels corresponding to the experimentally obtained spectrum were looked for with changing  $\theta$  and  $\lambda$  as parameters and the best fit was found in case of  $\theta = 90^\circ$  and  $\lambda = -0.75$ . Figure 5 shows the energy levels of the excited and ground

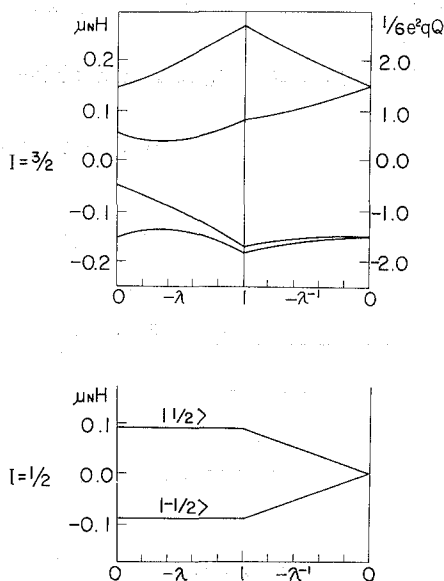


Fig. 5. Energy level diagram of Fe<sup>57</sup> excited state for  $\theta = 90^\circ$  as a function of  $\lambda$ . Here  $\lambda$  is the ratio of quadrupole interaction energy to Zeeman one.  $\theta$  is the angle between magnetic field axis and electric field axis.

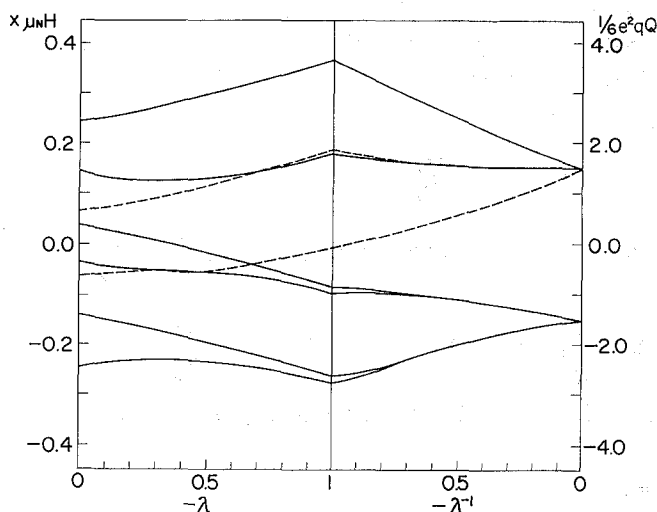


Fig. 6.  $\lambda$  dependence of the Mössbauer transition energies for  $\theta=90^\circ$ .

state for  $\theta=90^\circ$ . The number of possible Mössbauer transitions between ground and excited state is eight in contrast with six of usual case, because the levels of the excited state are no longer pure ones. In this case some of eight absorption lines approach to each other and nearly four absorption groups can be formed as shown in Fig. 6.

To confirm the assignment of transitions and energy levels mentioned above, transition intensity must be calculated. Therefore, the eigen functions for  $\theta=90^\circ$ ,  $\lambda=-0.75$ , were calculated by using equation (1), (3), (4) and (5). For  $\lambda=-0.75$ , the calculated eigen functions and energy levels are shown with the Mössbauer transitions in Fig. 7. In the same figure, the dotted lines shows the forbidden transition specially in pure state ( $\lambda=0$ ).

The relative intensity<sup>5)</sup> of gamma magnetic transition from initial state  $|E_i\rangle$

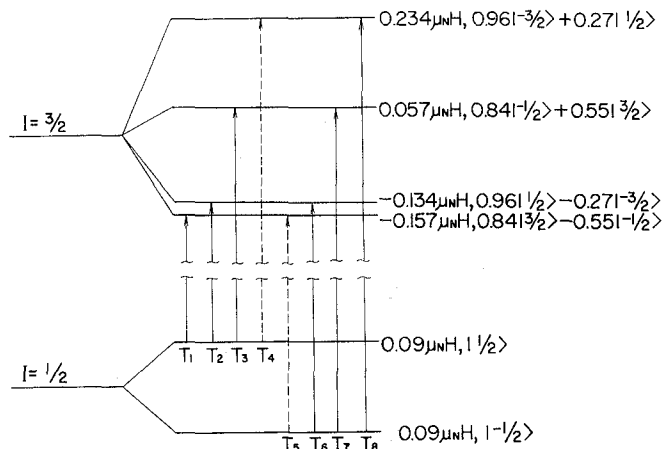


Fig. 7. Energy levels for the ground and excited state and Mössbauer transition of  $\text{Fe}^{57}$  for  $\lambda=-0.75$  and  $\theta=90^\circ$ . Also shown are the calculated eigen function for each levels.

to final state  $|E^f\rangle$  are shown for polycrystalline samples:

$$I = \frac{2|\chi_{\text{mag}}|^2}{2l+1} \sum_M |b_{ME^fE^i}^{(l)}|^2, \quad (7)$$

where  $\chi_{\text{mag}}$  is the reduced current matrix element and constant for all transitions and

$$b_{ME^fE^i}^{(l)} = \sum_{m_f m_i} (-1)^{m_f} \langle m_f | E^f \rangle^* \langle m_i | E^i \rangle (j_f, l, j_i; m_f, M, -m_i). \quad (8)$$

In equation (8),  $\langle m_f | E^f \rangle$  is coefficient in the expansion of mixed state  $|E^f\rangle$  in pure state  $|j_f m_f\rangle$  and identical with the coefficient in equation (4) and  $(j_f, l, j_i; m_f, M, -m_i)$  is the Clebsh-Gordan coefficient. When initial state is pure, equation (7) becomes simple form;

$$I = \frac{2}{2l+1} |\chi_{\text{mag}}|^2 \sum_{m_f} \langle m_f | E^f \rangle^2 (j_f, l, j_i; m_f, M, -m_i)^2. \quad (7')$$

In the case of Fe<sup>57</sup> Mössbauer transition, the values of  $l$ ,  $j_f$  and  $j_i$  must be replaced by 1, 3/2 and 1/2 respectively.

From equation (7'), relative intensity can be calculated for each transition at  $\lambda = -0.75$  using the eigen functions of Fig. 7. In Table 1, the values of calculated absorption energies and relative intensities are shown for  $\lambda = -0.75$ . The sign T<sub>1</sub>, T<sub>2</sub>..., T<sub>8</sub> is the same as those shown in Fig. 7 and velocity was normalized so that the energy separation between T<sub>1</sub> and T<sub>8</sub> was in accord with the experimental value, 7.73 mm/sec.

Table 1. Relative intensity and absorption energies calculated from eigen functions and energy levels of Fig. 7.

	Relative Intensity	Energy Separation from T <sub>8</sub> $\times \mu_N H$	Velocity mm/sec
T <sub>1</sub>	0.405	0.569	-1.85
T <sub>2</sub>	0.309	0.548	-1.58
T <sub>3</sub>	0.100	0.392	0.58
T <sub>4</sub>	0.173	0.368	0.88
T <sub>5</sub>	0.267	0.357	1.02
T <sub>6</sub>	0.012	0.180	3.42
T <sub>7</sub>	0.234	0.177	3.45
T <sub>8</sub>	0.470	0	5.88

By assuming that each transition has a Lorentz type function, a theoretical spectra is obtained for  $\lambda = -0.75$  as shown in Fig. 8. In the same figure, the broken lines show the Lorentz shape of each transition with half width, 0.4 mm/sec. By summing up them, the theoretical spectrum was obtained as shown by the solid line. Open circles represent the value of experiment. The agreement of experi-



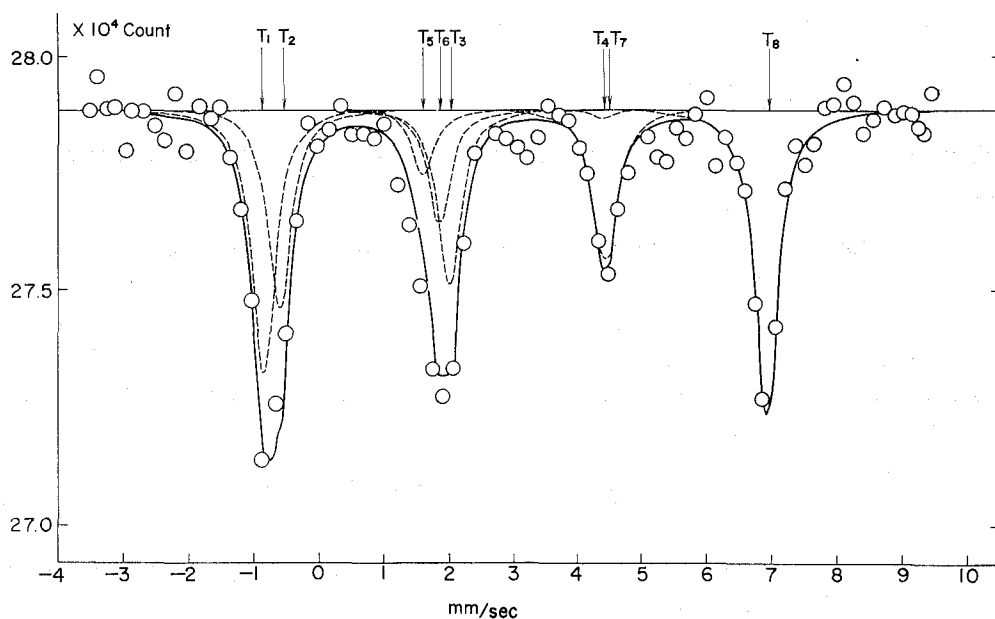


Fig. 8. Comparison of experimental data with the calculated spectrum using the value of Table 1. Theoretical spectrum for  $\lambda = -0.75$  was obtained by summarizing each Lorentz shape of absorption with half width 0.4 mm/sec.

mental spectrum with calculated one is much satisfactory.

Using the value of the energy separation between  $T_1$  and  $T_8$  and  $\lambda = -0.75$ , we can obtain 200 KOe for the magnetic hyperfine field, 3.06 mm/sec for  $1/2e^2qQ$  and 1.48 mm/sec for isomer shift. In the analysis of the Mössbauer spectrum at 4.2°K, it was assumed that asymmetric factor  $\eta$  is negligible. This assumption was verified to be valid due to the excellent agreement of experimental spectrum with calculated one. In consideration of the crystal structure of  $\text{Fe}(\text{OH})_2$ , it can be concluded that the electric field gradient is parallel to the c-axis and therefore spin axis of  $\text{Fe}(\text{OH})_2$  lies in the c-plane.

#### IV. CONCLUSION

Mössbauer effect of  $\text{Fe}(\text{OH})_2$  was studied in the antiferromagnetic and paramagnetic region.

The four lines splitting at 4.2°K was analyzed by the Parker's calculation and assignment of energy level was achieved. The magnetic hyperfine field, quadrupole splitting and isomer shift of  $\text{Fe}(\text{OH})_2$  at 4.2°K were derived as 200 KOe, 3.06 mm/sec and 1.48 mm/sec respectively.

The spin easy axis of  $\text{Fe}(\text{OH})_2$  at 4.2°K could be concluded to be perpendicular to the c-axis because the electric field gradient is perpendicular to the spin axis.

In the paramagnetic region,  $1/2e^2qQ$  and  $\delta$  were 3.00 mm/sec and 1.25 mm/sec and the temperature dependence of  $1/2e^2qQ$  was very small.

#### ACKNOWLEDGEMENT

The authors would like to express their sincere thanks to Dr. Mukoyama of Shimizu Laboratory, for discussing the probability of the Mössbauer transition.

#### REFERENCES

- (1) H. Miyamoto; *Bull. Inst. Chem. Res. Kyoto. Univ.*, **44**, 420 (1966).
- (2) T. Takada, Y. Bando, M. Kiyama and H. Miyamoto; *J. Phys. Soc. Japan*, **21**, 2726 (1966).
- (3) T. Takada, Y. Bando, M. Kiyama and H. Miyamoto; *ibid.*, **21**, 2745 (1966).
- (4) P.M. Parker; *J. Chem. Phys.*, **24**, 1096 (1956).
- (5) S.V. Karyagin; *Soviet Phys-Solid State*, **8**, 1287 (1966).